Current Biology 19, 50–53, January 13, 2009 ©2009 Elsevier Ltd All rights reserved DOI 10.1016/j.cub.2008.11.048

Report

Face Processing in the Chimpanzee Brain

Lisa A. Parr,[1,2,7,*] Erin Hecht,[1,4] Sarah K. Barks,[1,6] Todd M. Preuss,[1,3,7] and John R. Votaw[1,5]
[1]Yerkes National Primate Research Center
Atlanta, GA 30329
USA
[2]Division of Psychiatry and Behavioral Sciences
[3]Department of Pathology
School of Medicine
Emory University
Atlanta, GA 30322
USA
[4]Graduate Program in Neuroscience
[5]Department of Radiology
[6]Department of Anthropology
Emory University
Atlanta, GA 30322
USA
[7]Center for Behavioral Neuroscience
Atlanta, GA 30309
USA

Summary

Human face recognition involves highly specialized cognitive and neural processes that enable the recognition of specific individuals [1–5]. Although comparative studies suggest that similar cognitive processes underlie face recognition in chimpanzees and humans ([6–8] and Supplemental Data), it remains unknown whether chimpanzees also show face-selective activity in ventral temporal cortex. This study is the first to examine regional cerebral glucose metabolism with ^{18}F-flurodeoxyglucose positron emission tomography in chimpanzees after they performed computerized tasks matching conspecifics' faces and nonface objects (Supplemental Data). A whole-brain analysis comparing these two tasks in five chimpanzees revealed significant face-selective activity in regions known to comprise the distributed cortical face-processing network in humans, including superior temporal sulcus and orbitofrontal cortex [9–11]. In order to identify regions that were exclusively active during one task, but not the other, we subtracted a resting-state condition from each task and identified the activity exclusive to each. This revealed numerous distinct patches of face-selective activity in the fusiform gyrus that were interspersed within a large expanse of object-selective cortex. This pattern suggests similar object form topography in the ventral temporal cortex of chimpanzees and humans, in which faces may represent a special class of visual stimulus.

Results

Whole-Brain Analyses: Face versus Object

The first analysis revealed numerous brain regions that showed greater metabolic activity during the face-matching task when compared directly to the object-matching task by use of the contrast face minus object (see Table 1). Figure 1 illustrates face-selective activity in the posterior superior temporal sulcus (STS) and orbitofrontal cortex overlaid on a 3D rendering of a chimpanzee MRI. These regions comprise part of the distributed cortical network for face processing in humans [9–11]. Notably absent from this analysis was activity in the fusiform gyrus, the primary region where face-selective activity is found in humans when the comparable analysis is used [2, 3].

Whole-Brain and ROI Analyses: Face and Object versus Rest

A second analysis used a specific region of interest (ROI) approach to compare the proportion of task-specific voxels in each contrast (FR, face minus rest; OR, object minus rest; FO, face minus object) in both the fusiform gyrus and posterior STS of each individual subject (see Supplemental Results and Discussion available online). These means (+ SEM) are plotted in Figure 2. This illustrates that the fusiform gyrus had more face- and object-selective voxels than the posterior STS when compared to rest but that there were more face-selective voxels in the posterior STS than fusiform gyrus when compared to the object task.

These results are not surprising because the ventral temporal cortex in humans is known to be highly selective for a variety of object categories, not just faces [10, 12–16]. Moreover, the definitive face-selective region in humans, the fusiform face area, or FFA [2, 4], is small (about a cm^3), and its location is highly variable across individuals (see Supplemental Results and Discussion), so it is not surprising that the group analysis presented here did not identify a putative FFA in the chimpanzee brain, which is about one-third of the volume of the human brain. To overcome these issues, human studies use functional ROI approaches to first localize the FFA from surrounding object-selective cortex and then later compare neural responses to faces and control stimuli in these functionally defined regions [17]. Because the FDG-PET procedures used in the present study only allow for one experimental condition per scan, data are still being acquired that would enable a similar procedure to be implemented in the chimpanzee. The present data set, however, could conceivably be used as the functional localizer data for future studies.

A final analysis aimed to identify regions that were exclusively face selective or object selective across the whole brain in chimpanzees by comparing these conditions to the resting state, when subjects are awake and resting quietly in their home cage, which is known to activate social cognition networks in chimpanzees and humans [18, 19]. Figure 3 illustrates the location of face- and object-selective activity overlaid on several axial and coronal slices through the chimpanzee brain. According to the analysis, red regions show voxels that were significantly ($p < 0.05$) and uniquely active for the FR contrast but showed no activation in the OR contrast, and the yellow regions indicate voxels that were significantly and uniquely active for the OR contrast, showing no activation in the FR contrast. Figure 3 shows the location of face-selective activity to be tightly interspersed within a large

*Correspondence: lparr@emory.edu

Table 1. A List of Face-Selective Brain Regions in the Chimpanzee

Brain Region	Volume (mm^3)	p Value	Side of Activation
Dorsal primary motor/medial parietal cortex	460.60	0.001	L
Intraparietal sulcus	243.31	0.002	R
Parieto-occipital sulcus/posterior cingulate	218.23	0.003	Bilat
Anterior cingulate	188.93	0.005	R
Medial prefrontal cortex	179.55	0.006	L
Intraparietal sulcus	151.89	0.01	L
Middle STS/insula	121.42	0.019	L
Lateral primary motor cortex	112.98	0.023	L
Ventromedial orbitofrontal cortex/medial orbital cortex	101.26	0.03	R
Anterior cingulate	94.23	0.035	L
Posterior superior temporal sulcus (STS)	83.92	0.045	R
Posterior STS	80.17	0.05	L
Medial parietal cortex	80.17	0.05	L

A listing of brain regions identified in chimpanzees as being significantly more active during the face-matching compared to object-matching task ($p < 0.05$, one-tailed). This was derived by a whole-brain analysis including only clusters of two or more contiguous voxels, in which the volume of activation was > 20 mm^3.

object-responsive territory in the ventral temporal cortex, particularly the right fusiform gyrus. In addition to fusiform gyrus, face-selective activity was found in nucleus accumbens, superior temporal gyrus, posterior STS, supramarginal gyrus, posterior parietal cortex/angular gyrus, and the parieto-occipital sulcus. Additional object-selective activity was found in precentral gyrus, insula, and thalamic nuclei. Both contrasts activated nonoverlapping regions in ventromedial orbitofrontal cortex, inferior frontal gyrus, parahippocampal cortex, and the calcarine fissure.

These regions may represent part of a distributed neural system for face processing in chimpanzees, as proposed in humans, where the initial visual analysis of faces activates regions in the occipitotemporal cortex, and then additional processing may take place in the fusiform gyrus, STS, and extended regions [9]. Although the data from this study do not permit definitive demonstration of a chimpanzee FFA homolog, face-selective regions were found to be distributed throughout the brain, particularly in the right posterior fusiform gyrus, which were tightly interspersed within regions of object-selective cortex. This is consistent with the existence of a specific subregion within the ventral visual cortex of chimpanzees for processing unique classes of objects: faces.

Discussion

In order to understand whether a particular behavior, such as expertise in face recognition, represents a unique specialization in humans, comparative data are essential. Previous behavioral studies in chimpanzees have demonstrated many of the same cognitive specializations for face processing as humans, such as rapid individuation of faces [6], species-specific face-inversion effects [7], and utilization of second-order relational information [8]. Behavioral evidence for similar face expertise in monkeys has not been strongly established ([20], but see [21]). Moreover, whereas monkeys have a series of interconnected face-selective brain regions, these patches lie along the lateral aspect of the temporal lobe, within the STS and on the adjacent inferior temporal convexity [22–26], not in the ventromedial aspect of the posterior temporal lobe where face-selective activity is primarily observed in humans and is reported here in chimpanzees. Thus, there is currently no strong evidence to suggest that macaque face selectivity is in a region that could be considered homologous to the fusiform gyrus. The functional topography of these areas, however, appears quite similar in all species in that the face-selective regions are embedded within object-selective cortex [22].

Thus, the data presented here support similar neural substrates for face processing in chimpanzees and humans

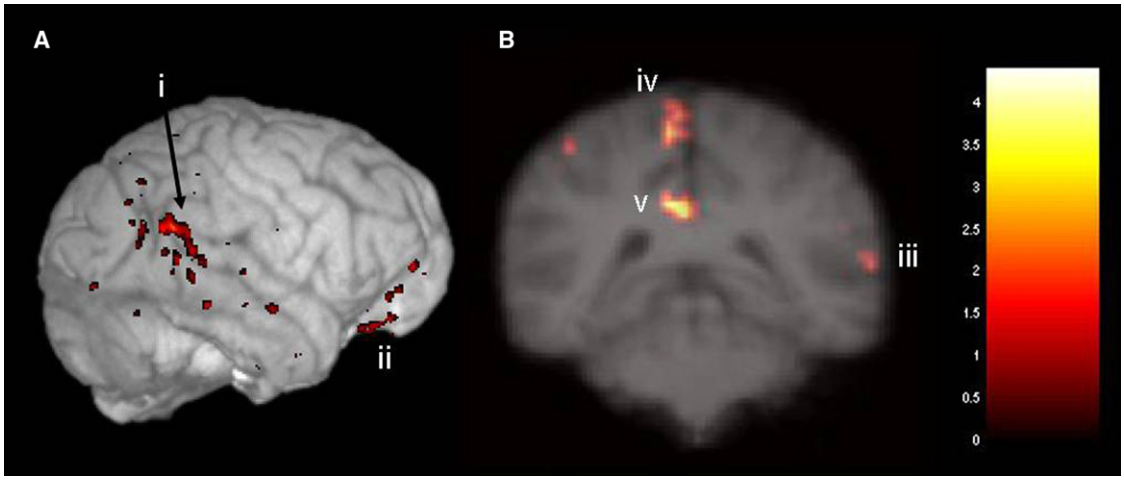

Figure 1. Face-Selective Brain Regions in Chimpanzees

Figure 1 illustrates the results of a whole-brain analysis comparing metabolic brain activity during the face- versus object-matching task ($p < 0.05$, uncorrected).

(A) Face-selective activations in the right posterior STS (i) and orbitofrontal cortex (ii) overlaid on a 3D reconstruction of the average chimpanzee MRI (chimplate).

(B) Face-selective activations in right posterior STS (iii), left primary motor/medial parietal cortex (iv), and posterior cingulate (v) overlaid on a coronal slice of the chimplate.

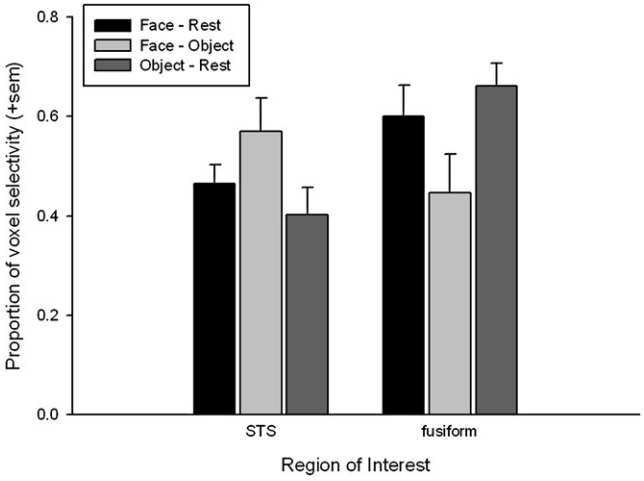

Figure 2. Proportion of Face- and Object-Selective Voxels in Specific Brain Regions

The mean (+ SEM) proportion of face- and object-selective voxels in the fusiform gyrus and posterior STS identified with the following contrasts: face minus rest (FR), object minus rest (OR), and face minus object (FO).

distributed across the whole brain and, specifically, by revealing face-related activity in the fusiform gyrus, orbitofrontal cortex, and posterior STS. Collectively, these similarities and differences suggest that the last common ancestor of macaques, chimpanzees, and humans may have shared a set of neurocognitive mechanisms used to process faces and other relevant visual stimuli but that additional neural mechanisms evolved in the common ancestry of chimpanzees and humans, pushing these regions into ventromedial temporal cortex and enabling greater expertise in analyzing and individuating faces. Further studies will be needed before the evolutionary details of these specializations become clearer, such as whether these skills are present in other great apes.

Experimental Procedures

Subjects and Procedure

Five adult chimpanzees (three males, 14–18 years of age) participated in these studies. All subjects had prior experience matching faces via computerized tasks (Supplemental Results and Discussion) [6–8]. The stimuli used in this study were novel photographs of individuals who were personally unfamiliar to the subjects and clip art objects that did not show any faces or face-like images (Supplemental Results and Discussion).

Prior to each task, the subject was given a 15 mCi dose of [^{18}F]-FDG (2–3 ml volume mixed in ~50 ml of Kool-Aid sweetened with Splenda). Subjects then began working on either the face-matching task or the object-matching task, performing without interruption for the entire [^{18}F]-FDG uptake period, ~45–60 min, when the absorption of [^{18}F]-FDG into the brain begins to asymptote. Subjects were then anesthetized and transported to the Emory University Hospital's Center for Positron Emission Tomography, where they received a 3D whole-brain scan with a Siemens High Resolution Research Tomograph under propofol anesthesia (10 mg/kg/hr) following established procedures ([27, 28], Supplemental Results and Discussion).

Image Processing and Data Analysis

Each subject's PET scan (face, object, and rest conditions) was coregistered to its own MRI. These were converted to a binary mask and applied to the coregistered PET scans to effectively strip away nonbrain information. Each stripped and coregistered PET scan was then normalized to its average whole-brain activity so that regional cerebral glucose metabolism (rCGM) could be compared across conditions and between subjects. These scans were then spatially normalized to an average chimpanzee MRI template (chimplate) (Supplemental Results and Discussion), and these were analyzed with repeated-measures ANOVAs in SPM5 where task condition was the within-subject factor. Subsequent t tests were used to identify which brain regions were significantly more active during one task compared to another. The first analysis compared the face-matching and object-matching tasks directly ($p < 0.05$) by using the contrast face minus object (FO). This analysis used a more liberal threshold than is typically assessed in neuroimaging studies, which was motivated by the small sample

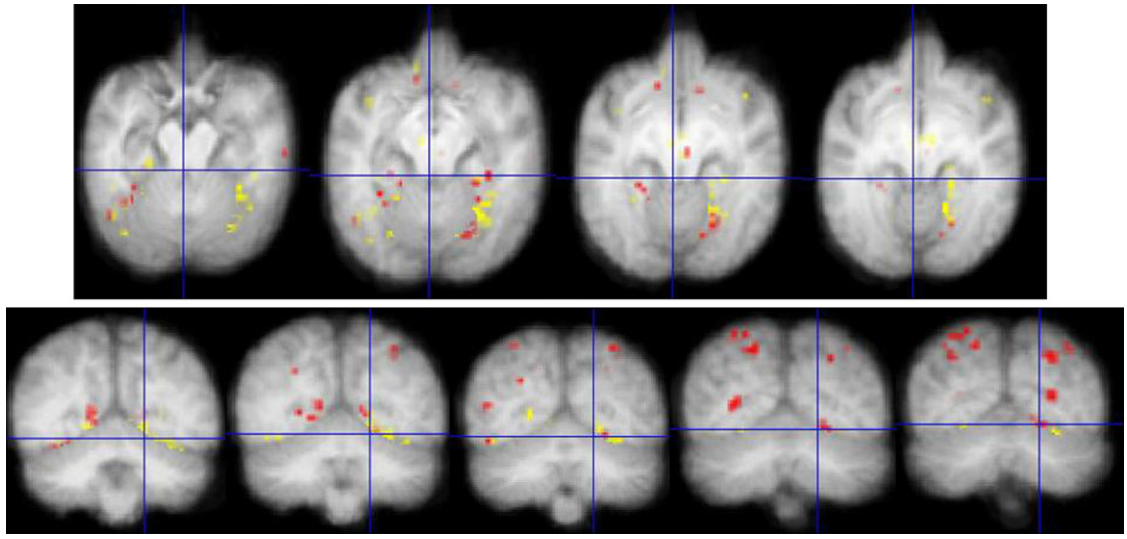

Figure 3. The Location of Unique Face- and Object-Selective Activity in the Chimpanzee Brain

The results of repeated-measures ANOVA in SPM5 showing the location of face- and object-selective ($p < 0.05$) activity compared to rest were first binarized and then added to form the union of these results (FR + OR). Each binarized condition was then subtracted from the binarized union to reveal regions that were uniquely face selective (bin[FR + OR] − binOR) or uniquely object selective (bin[FR + OR] − binFR). Red patches show voxels that were significantly more active in the FR contrast but showed no activation in the OR contrast. Yellow regions show voxels that were significantly more active during the OR contrast but showed no activation in the FR contrast. These activations are overlaid on an average chimpanzee MRI brain in the axial (top row) and coronal (bottom row) planes. Images are in neurological convention (left is left).

size, to provide descriptive analysis of the extended neural regions activated across the whole brain.

Second, for each contrast—face minus rest (FR), object minus rest (OR), and face minus object (OR)—the proportion of task-specific voxels was calculated with an ROI-based analysis. The ROIs included were the fusiform gyrus and the posterior STS (see Supplemental Results and Discussion). The task-specific activity in each ROI was calculated by dividing the number of positive voxels by the size of the individual ROI. Thus, for the contrast FR, positive voxels were those more active for faces compared to rest.

Finally, the face- and object-selective topography of the chimpanzee brain was analyzed by identifying voxels that were unique to each condition when compared to a resting-state baseline. Regions that were significantly ($p < 0.05$) more face- (FR) and object-selective (OR) when compared to rest were identified with SPM5. These t-map images were then binarized and combined to produce an image showing the union of activity in the two contrasts (binFR + binOR). Each of the original binarized t-map images, either binFR or binOR, were then subtracted from the binarized union, revealing the regions that were uniquely active in each individual contrast. In this manner, regions of activity that were shared by each contrast were effectively removed, resulting in activity that was inclusive only of regions unique to that contrast. Unique "face-selective" regions were plotted from the t-map resulting from (bin[FR + OR] − binOR), and unique "object-selective" regions were plotted from the t-map resulting from (bin[FR + OR] − binFR). These results should be interpreted cautiously because the binarizing procedure may overinflate true differences between the tasks. (A voxel that is slightly greater in condition A compared to condition B, e.g., 0.5 versus 0.4, when binarized becomes assigned to condition A. Thus, some voxels that were identified as selective for condition A, but not also selective for condition B, may indeed be only slightly more selective for A. The same inflation would apply for voxels identified as selective for condition B, but not also selective for condition A.)

Supplemental Data

Supplemental Data include Supplemental Results and Discussion, one table, and six figures and can be found with this article online at http://www.current-biology.com/supplemental/S0960-9822(08)01566-2.

Acknowledgments

This investigation was supported by RR-00165 from the National Institutes of Health/National Center for Research Resources to the Yerkes National Primate Research Center (YNPRC); R01-MH068791 to L.A.P.; NIGMS T32 GM008605 training grant to E.H.; James S. McDonnell Foundation grant 21002093 to T.M.P.; and The Center for Behavioral Neuroscience IBS#9876754, a Science and Technology Center Program of the National Science Foundation. The Yerkes National Primate Research Center is fully accredited by the American Association for Accreditation of Laboratory Animal Care. Helpful input was provided by Nancy Kanwisher and three anonymous reviewers. Thanks to Jim Rilling for providing the resting-state brain scans, Sheila Sterk for animal assistance, Delicia Votaw and Margie Jones for scanning assistance, and the veterinary and animal care staff at the YNPRC.

Received: August 26, 2008
Revised: November 13, 2008
Accepted: November 14, 2008
Published online: December 18, 2008

References

1. Maurer, D., Grand, R.L., and Mondloch, C.J. (2002). The many faces of configural processing. Trends Cogn. Sci. *6*, 255–260.
2. Kanwisher, N., McDermott, J., and Chun, M.M. (1997). The fusiform face area: A module in human extrastriate cortex specialized for face perception. J. Neurosci. *17*, 4302–4311.
3. McCarthy, G., Puce, A., Gore, J.C., and Allison, T. (1997). Face-specific processing in the human fusiform gyrus. J. Cogn. Neurosci. *9*, 605–610.
4. Yovel, G., and Kanwisher, N. (2004). Face perception: Domain specific, not process specific. Neuron *44*, 889–898.
5. Gauthier, I., Tarr, M.J., Moylan, J., Skudlarski, W., Core, J.C., and Anderson, A.W. (2000). The fusiform "face area" is part of a network that processes faces and the individual level. J. Cogn. Neurosci. *12*, 495–504.
6. Parr, L.A., Winslow, J.T., Hopkins, W.D., and de Waal, F.B.M. (2000). Recognizing facial cues: Individual recognition in chimpanzees (Pan troglodytes). J. Comp. Psychol. *114*, 47–60.
7. Parr, L.A., Dove, T.A., and Hopkins, W.D. (1998). Why faces may be special: Evidence for the inversion effect in chimpanzees (Pan troglodytes). J. Cogn. Neurosci. *10*, 615–622.
8. Parr, L.A., Heintz, M., and Akamagwuna, U. (2006). Three studies of configural face processing by chimpanzees. Brain Cogn. *62*, 30–42.
9. Haxby, J.V., Hoffman, E.A., and Gobbini, M.I. (2000). The distributed human neural system for face perception. Trends Cogn. Sci. *4*, 223–233.
10. Haxby, J.V., Gobbini, M.I., Furey, M.L., Ishai, A., Schouten, J.L., and Pietrini, P. (2001). Distributed and overlapping representation of faces and objects in ventral temporal cortex. Science *293*, 2425–2430.
11. Ishai, A., Schmidt, C.F., and Boesiger, P. (2005). Face perception is mediated by a distributed cortical network. Brain Res. Bull. *67*, 87–93.
12. Kreiman, G., Koch, C., and Fried, I. (2000). Category specific visual responses of single neurons in the human medial temporal lobe. Nat. Neurosci. *3*, 946–953.
13. Ishai, A., Ungerleider, L.G., Martin, A., Schouten, J.L., and Haxby, J.V. (1999). Distributed representation of objects in the human ventral visual pathway. Proc. Natl. Acad. Sci. USA *96*, 9379–9384.
14. Gerlach, C., Law, I., Gade, A., and Paulson, O.B. (2000). Categorization and category effects in normal object recognition: A PET study. Neuropsychologia *38*, 1693–1703.
15. Goodale, M.A., and Milner, A.D. (1992). Separate visual pathways for perception and action. Trends Neurosci. *15*, 20–25.
16. Grill-Spector, K., Kushnir, T., Hendler, T., Edelman, S., Itzchak, Y., and Malach, R. (1998). A sequence of object-processing stages revealed by fMRI in the human occipital lobe. Hum. Brain Mapp. *6*, 316–328.
17. Saxe, R., Brett, M., and Kanwisher, N. (2006). Divide and conquer: In defense of functional localizers. Neuroimage *30*, 1088–1096.
18. Rilling, J.K., Barks, S.K., Parr, L.A., Preuss, T.M., Faber, T.L., Pagnoni, G., Bremner, J.D., and Votaw, J.R. (2007). A comparison of resting state brain activity in humans and chimpanzees. Proc. Natl. Acad. Sci. USA *104*, 17146–17151.
19. Schilbach, L., Eickhoff, S.B., Rotarska-Jagiela, A., Fink, G.R., and Vogeley, K. (2008). Minds at rest? Social cognition as the default mode of cognizing and its putative relationship to the "default system" of the brain. Conscious. Cogn. *17*, 457–467.
20. Parr, L.A., Heintz, M., and Pradhan, G. (2008). Rhesus monkeys (Macaca mulatta) lack expertise in face processing. J. Comp. Psychol. *122*, 390–402.
21. Dahl, C.D., Logothetis, N.K., and Hoffman, K.L. (2007). Individuation and holistic processing of faces in rhesus monkeys. Proc. Biol. Sci. *274*, 2069–2076.
22. Tsao, D.Y., Freiwald, W.A., Knutsen, T.A., Madndeville, J.B., and Tottell, R.B.H. (2003). Faces and objects in macaque cerebral cortex. Nat. Neurosci. *6*, 989–995.
23. Tsao, D.Y., Freiwald, W.A., Tootell, R.B.H., and Livingstone, M.S. (2006). A cortical region consisting entirely of face-selective cells. Science *311*, 670–674.
24. Pinsk, M.A., DeSimone, K., Moore, T., Gross, C.G., and Kastner, S. (2005). Representations of faces and body parts in macaque temporal cortex: A functional MRI study. Proc. Natl. Acad. Sci. USA *102*, 6996–7001.
25. Perrett, D.I., Mistlin, A.J., Chitty, A.J., Smith, P.A.J., Potter, D.D., Borennimann, R., and Harries, M.H. (1988). Specialized face processing and hemispheric asymmetry in man and monkey: Evidence from single unit and reaction time studies. Behav. Brain Res. *29*, 245–258.
26. Hoffman, K.L., Gothard, K.M., Schmid, M.C., and Logothetis, N.K. (2007). Facial-expression and gaze-selective responses in the monkey amygdala. Curr. Biol. *17*, 766–772.
27. Phelps, M.E., Huang, S.C., Hoffman, E.J., Selin, C., Sokoloff, L., and Kuhl, D.E. (1979). Tomographic measurement of local cerebral glucose metabolic rate in humans with (F-18)2-fluoro-2-deoxy-D-glucose: Validation of method. Ann. Neurol. *6*, 371–388.
28. Phelps, M.E., and Mazziotta, J.C. (1985). Positron emission tomography: human brain function and biochemistry. Science *228*, 799–809.

Current Biology, *Volume 19*

Supplemental Data

Face Processing in the Chimpanzee Brain

Lisa A. Parr, Erin Hecht, Sarah K. Barks, Todd M. Preuss, and John R. Votaw

Supplemental Results and Discussion

Face expertise in chimpanzees

Previous studies in our lab have demonstrated that chimpanzees, as opposed to monkeys, are highly skilled at discriminating unfamiliar conspecifics' faces. These studies have been conducted using computerized testing systems that present faces in a matching-to-sample (MTS) format (Figure S1). When first learning to discriminate unfamiliar conspecifics' faces in our lab, chimpanzees performed above chance on day one of testing. In contrast, rhesus monkeys with the same level of computerized training required over 100 presentations before their performance exceeded chance levels (Parr et al., 2000). A more complex version of the MTS task was then used to examine the recognition of specific individuals from faces. In these tasks, two different photographs of the same individual were presented as the matching pair, and a third picture of a different individual was used as the nonmatch. Thus, matching requires recognizing the facial configurations of the individuals and not specific features of the photographs. In these individual recognition (IR) tasks, chimpanzees also performed above chance within a single testing session after having seen each trial twice, whereas monkeys required an additional 60 trials before they performed above chance (Parr et al., 2000). This species difference was confirmed more recently using a new group of rhesus monkeys working on face recognition tasks in our lab. They also required many trials before they successfully learned to discriminate between different photographs of unfamiliar conspecifics and consistently failed to show improvement in their

performance when novel examples were presented (Parr, Heintz & Pradhan, 2008). Thus, monkeys and chimpanzees show fundamental differences both learning to individuate faces and continuing to perform similar tasks with novel faces.

The face-inversion effect refers to the performance deficit that occurs when faces are presented upside down. This is believed to occur because faces are typically processed using the configuration of facial features and this basic configuration is disrupted when faces are inverted (Valentine, 1988). Similar effects are not observed for nonface stimuli. When tested on the face-inversion effect, chimpanzees show selective impairments only for the categories of faces that they have some familiarity with, such as conspecifics' and human faces, but not unfamiliar face categories, or any nonface category (Parr, Dove & Hopkins, 1998). This is consistent with the results on the face-inversion effect in chimpanzees from another lab using slightly different methods (Tomonaga, 2007). Data from rhesus monkeys, both from our lab and others', have failed to show consistent face-inversion effects, suggesting that monkeys are not relying on unique configurations of facial features to discriminate among individuals. While some studies have shown evidence of orientation-specific processing in monkeys (Neiworth et al., 2007; Overman & Doty, 1982; Tomonaga, 1994 and Vermeire & Hamilton, 1998), others have failed to show these orientation-specific effects (Bruce, 1982; Dittrich, 1990; Gothard et al., 2004; Parr et al., 1999; Parr, Heintz & Pradhan, 2008; Rosenfeld & van Hoesen, 1979; Weiss et al., 2001).

Finally, chimpanzees, like humans, show sensitivity to the 2nd-order configural features in faces, that is, the spacing of features with regards to one another, which has not been demonstrated in monkeys (Parr et al., 2006; Parr, Heintz & Pradhan, 2008). Collectively, chimpanzees and monkeys appear to process faces quite differently, with chimpanzees showing

many of the same cognitive specializations for face processing as humans, and monkeys showing weak or inconsistent evidence for these patterns of expertise.

Stimuli: Faces and Objects

In this study, subjects performed a face matching task and a clip-art (object) matching task (Figure S1). These task sessions were separated by at least 2 weeks and the order was counterbalanced across subjects. Over 100 examples of images from each category were used. Photographs of chimpanzee faces showed only unfamiliar individuals and clip-art images were downloaded from internet sites. Clip art did not show any faces or face-like images. Other photographs of the same chimpanzees, however, had been presented numerous times in previous experiments, so although the subjects were not personally familiar with these individuals, they had seen their pictures before. In this experiment, however, all of the actual photographs used were novel. The MTS software randomly selected two images for each trial, where the correct pair was identical images and the nonmatch/foil image was another example from that same category, either another face or another clip art. No single image was repeated before all had been seen at least once. Performance data during each task session are listed in Table S1. The trial numbers confirm that even in the most prolific subjects, during a 45-60 minute testing session they saw each image no more than seven times.

The Matching-to-Sample Task

These studies were conducted using a computerized-joystick matching-to-sample (MTS) task. This has been the main task in the lab for studying social cognition and face recognition in chimpanzees (see Parr et al., 2000; Parr et al., 2006). The chimpanzees involved in these studies had considerable experience matching unfamiliar conspecifics' faces using this format, as described above, so no additional training was required and subjects readily participated on a

voluntary basis (food restriction was required for anesthetic protocol but subjects were rewarded during the tasks on approximately 30% of their correct trials with sugar-free Kook-Aid™). According to the MTS procedure, a computer is wheeled to the front of subjects' home cage and a joystick is positioned on the cage mesh so that the stick protrudes horizontally through the mesh. Subjects have been trained to control the movements of a cursor on the computer screen by manipulating the joystick in an isomorphic manner. At the beginning of a trial, a single image (the sample) appears on the computer screen on a black background. Subjects orient to this by contacting it with the joystick-controlled cursor. After this, the sample clears the screen and two comparison images appear on the monitor, equidistant from the sample but on the opposite wall of the computer monitor. One of these comparisons matches the sample (the target), and the other (the foil) is a different image from the same category, either another face or another clip art object. This format is referred to as sequential MTS, as there is a very short delay between the orienting response to the sample and the presentation of the two comparison images. Subjects must contact the image that matches the sample by contacting it with the joystick-controlled cursor. After this, they receive a small food reward (squirt of sugar-free juice) and a short inter-trial interval (ITI). If their response is incorrect, i.e. they select the nonmatching foil image, they are not food-rewarded and a slightly longer ITI follows. After this, the next trial proceeds.

Description of Fusiform Gyrus and Superior Temporal Sulcus ROIs

Two regions of interest were identified for use in the second analysis that compared the proportion of voxels specific for each contrast: face minus rest, object minus rest and face minus object. These included grey matter only and were drawn on each individual subjects' MRI scan using MRIcro (http://www.sph.sc.edu/comd/rorden/mricro.html). These were then saved as

image files and imported into SPM5 where they were converted to binary masks and applied to each of the three contrasts to extract the activity in only those regions.

The fusiform gyrus ROI was defined medially by the collateral sulcus (COS) and laterally by the occipitotemporal sulcus (OTS) in the coronal plane. The anterior boundary was defined in the coronal plane as the anterior-most section in which the temporal horn of the lateral ventricle can be seen to be continuous with the body of the lateral ventricle. The posterior boundary was defined in the coronal plane by a consistent landmark in the calcarine fissure, the point at which the prominent internal bend evident at the anterior levels of the fissure is replaced by a nearly straight configuration (see Figure S2A). The fusiform gyrus ranged in size from 2280 to 3376 mm^3.

The posterior STS ROI was also drawn in the coronal plane. The anterior border was defined in the plane corresponding to the posterior limit of the insular island. The posterior border was defined in the plane where the STS hooks superiorly and anteriorly, a location clearly evident on the lateral surface of the brain in 3D reconstruction (see Figure 2B). The posterior STS ROI ranged in size from 5079 to 6859 mm^3.

Variability of FFA Location in Published Studies

Neuroimaging studies on human face perception typically use a functional region-of-interest (ROI) approach. This is largely due to the fact that the specific location of the fusiform face area (FFA) is highly variable across individual subjects and across published studies (Saxe et al., 2006). Figure S3 shows this variability plotted on a schematized 3-dimensional human brain and, as a point of comparison, Figure S4 shows the location of the top 5% of face > object voxels in the fusiform gyrus of each chimpanzee. Left side shows the left hemisphere.

According to this method, an initial set of scans are conducted to functionally identify face-selective regions in the fusiform gyrus compared to a control task. These regions then serve as the functional ROIs to analyze a new data set. Because FDG-PET enables only a single task condition to be presented in a scanning session, this technique is much more time consuming than fMRI, where repeated conditions can be presented within a session. Subjects additionally require some time between scanning sessions to recover from the anesthetic protocol, so the scans obtained per subject are separated by a minimum of several weeks. To date, only one set of scans (face-matching, object-matching and resting-state) has been performed on each subject. A second series of scans are underway and should be completed early in 2009.

MRI & PET Scan Acquisition & Template

The Emory University Center for Positron Emission Tomography, in collaboration with the Yerkes National Primate Research Center, has many years experience conducted imaging sequences on nonhuman primates using oral-dosing procedures (Figure S5). Once the chimpanzees were positioned in the scanner bed (Figure S6), an initial transmission scan was performed using a Cs-137 point source. The attenuation image was reconstructed, segmented into air, tissue (water) and bone, and the Cs-137 attenuation coefficients were replaced with the appropriate 511 keV attenuation coefficients. Attenuation correction factors were determined by fore projecting this image. Emission data was collected for 15 min in list mode. The data were then rebinned into a 3D sinogram (span 9). Scatter was estimated using the single scatter source method of Watson and colleagues (1996) with slice by slice consistency constraints. Emission images were reconstructed iteratively using the 3D OP-OSEM algorithm supplied by the manufacturer and implemented on a 12 node PC cluster.

Magnetic resonance imaging (MRI) scans were acquired from all subjects prior to the onset of these PET studies by the Imaging Core of the Yerkes National Primate Research Center using a 3T Siemens scanner and a T1-weighted MP-RAGE sequence (TR= 2300 ms, TE = 4.4 ms, TI=1100 ms, flip angle = 8, 3 signals averaged) with a 0.63 x 0.63 x 0.60 mm voxel size. Subjects were anesthetized directly in the home cage using Telazol® (4-5 mg/kg, i.m.) and transported to the Imaging suite at the Yerkes National Primate Research Center. Anesthesia was maintained during the scan with intravenous propofol (10 mg/kg/hr) by veterinarian staff and monitored continually throughout the 30 minute scan. Subjects were positioned supine on the scanner bed and their head was fitted inside a standard human head coil. After a short orientation scan, the T1 sequence was started. These images were reconstructed into a 3D volume, the skulls were stripped from the images using MRIcro (http://www.sph.sc.edu/comd/rorden/mricro.html) to reveal only brain tissue. These were then used for coregistration during the PET analyses.

Additionally, a set of 8 chimpanzee MRIs obtained using identical scan parameters from additional subjects living at the Yerkes Primate Center were used to create a spatially normalized MRI chimpanzee template. This was created by Dr. John Votaw by binary process of successive averaging. Initially, images were randomly paired and these pairs, consisting of randomly assigned source and target images, were registered to each other. Affine scaling, rotations, and translations were permitted (12 degrees of freedom). Once the registration was determined, half of the transformation was applied to the source image and its inverse applied to the reference image to create a composite image that is, in some sense, half way between the two initial images. By creating composite images in this way, no particular chimpanzee's anatomy played a greater role in the final composite than any other. Next, the composite images were paired off and the process repeated. This process was repeated until a single composite image was formed.

By forming the average in this way, all subjects contributed equally to the final standard, which we termed the “chimplate.”

Table S1. Performance of Subjects on the Face- and Object-Matching Tasks, Including Number of Trials Completed, Mean Percentage Correct, and Average Time in Seconds before They Initiated a New Trial

	Face-matching task			Object-matching task		
Subject	Trials	% correct	latency	Trials	% correct	latency
Jarred	350	87.14	2.98	252	90.10	4.41
Faye	141	82.30	12.04	213	95.30	4.60
Scott	266	77.10	6.23	248	83.50	6.84
*Katrina	280	n/a	n/a	332	97.90	4.00
*Patrick	n/a	n/a	n/a	272	98.50	6.90
Mean	259.25	82.18	7.08	263.40	93.06	5.35

* Computer error prevented the collection of the face-matching data for Katrina and Patrick.

Studies included in Figure S3

Clark, V.P., Keil, K., Maisog, J.M., Courtney, S., Ungerleider, L.G. and Haxby, J.V. (1996). Functional magnetic resonance imaging of human visual cortex during face matching: a comparison with positron emission tomography. *Neuroimage, 1*, 1-15.

Druzgal, T.J. and D'Esposito, M. (2001). A neural network reflecting decisions about human faces. *Neuron, 32*, 947-955.

Druzgal, T.J. and D'Esposito, M. (2001). Activity in fusiform face area modulated as a function of working memory load. *Brain Res Cogn Brain Res., 3*, 355-364.

Ganel, T., Valyear, K.F., Goshen-Gottstein, Y. and Goodale, M.A. (2005). The involvement of the "fusiform face area" in processing facial expression. *Neuropsychologia, 43*, 1645-1654.

Gauthier, I., Tarr, M. J., Moylan, J., Skudlarski, W., Core, J. C., & Anderson, A. W. (2000). The fusiform "face area" is part of a network that processes faces and the individual level. *J. Cog. Neurosci., 12*, 495-504.

Gauthier, I., Skudlarski, P., Gore, J. C., & Anderson, A. W. (2000). Expertise for cars and birds recruits brain areas involved in face recognition. *Nature Neurosci., 3*, 191-197.

Gobbini, M. I., & Haxby, J. V. (2006). Neural response to the visual familiarity of faces. *Brain Res. Bull., 71*, 76-82.

Grill-Spector, K., Knouf, N., & Kanwisher, N. (2004). The fusiform face area subserves face perception, not generic within-category identification. *Nature Neurosci., 7*, 555-562.

Grill-Spector, K., Sayres, R. and Ress, D. (2006). High-resolution imaging reveals highly selective nonface clusters in the fusiform face area. *Nat. Neurosci., 9*, 1177-1185.

Haxby, J.V., Horwitz, B., Ungerleider, L.G., Maisog, J.M., Pietrini, P. and Grady, C.L. (1994). The functional organization of human extrastriate cortex: a PET-rCBF study of selective attention to faces and locations. *J. Neurosci., 11*, 6336-6353.

Haxby, J. V., Ungerleider, L. G., Horwitz, B., Maisog, J. M., Rapoport, S. I., & Grady, C. L. (1996). Face encoding and recognition in the human brain. *PNAS, 93*, 922-927.

Haxby, J. V., Ungerleider, L. G., Clark, V. P., Schouten, J. L., Hoffman, E. A., & Martin, A. (1999). The effect of face inversion on activity in human neural systems for face and object perception. *Neuron, 22*, 189-199.

Ishai, A., Haxby, J.V. and Ungerleider, L.G. (2002). Visual imagery of famous faces: effects of memory and attention revealed by fMRI. *Neuroimage, 17*, 1729-1741.

Katanoda, K., Yoshikawa, K., & Sugishita, M. (2000). Neural substrates for the recognition of newly learned faces: a functional MRI study. *Neuropsychologia, 38*, 1616-1625.

McCarthy, G., Puce, A., Gore, J. C., & Allison, T. (1997). Face-specific processing in the human fusiform gyrus. *J. Cog. Neurosci., 9*, 605-610.

Puce, A., Allison, T., Asgari, M., Gore, J. C., & McCarthy, G. (1996). Differential sensitivity of human visual cortex to faces, letterstrings, and textures: a functional magnetic resonance imaging study. *J. Neurosci., 16*, 5205-5215.

Vuilleumier, P., Armony, J. L., Driver, J., & Dolan, R. J. (2001). Effects of attention and emotion on face processing in the human brain: An event-related fMRI study. *Neuron, 30*, 829-841.

Additional References

Bruce, C. (1982). Face recognition by monkeys: absence of an inversion effect. Neuropsychologia, 20, 515-521.

Dittrich, W. (1990). Representation of faces in longtailed macaques (Macaca fascicularis). Ethol., 85, 265-278.

Gothard, K. M., Erickson, C. A. & Amaral, D. G. (2004). How do rhesus monkeys (Macaca mulatta) scan faces in a visual paired comparison task? Anim. Cog., 7, 25-36.

Overman, W. H. & Doty, R. W. (1982). Hemispheric specialization displayed by man but not macaques for analysis of faces. Neuropsychologia, 20, 113-128.

Neiworth, J. J., Hassett, J. M. & Sylvester, C. J. (2007). Face processing in humans and new world monkeys: the influence of experiential and ecological factors. Anim. Cog., 10, 125-134.

Parr, L.A., Winslow, J.T., Hopkins, W.D. and de Waal, F.B.M. (2000). Recognizing facial cues: Individual recognition in chimpanzees (Pan troglodytes). J. Comp. Psychol., 114, 47-60.

Parr, L.A., Winslow, J. T. and Hopkins, W. D. (1999). Is the inversion effect in rhesus monkeys face specific? Anim. Cog., 2, 123-129.

Parr, L.A., Heintz, M. and Akamagwuna, U. (2006). Three studies of configural face processing by chimpanzees. Brain and Cog., 62, 30-42.

Parr, L.A., Heintz, M. and Pradhan, G. (2008). Rhesus monkeys lack face expertise. J. Comp. Psychol., 122, 390-402.

Parr, L.A., Dove, T.A. and Hopkins, W.D. (1998). Why faces may be special: Evidence for the inversion effect in chimpanzees (Pan troglodytes). J. Cog. Neurosci., 10, 615-622.

Rosenfeld, S. A. & Van Hoesen, G. W. (1979). Face recognition in the rhesus monkey. Neuropsychologia, 17, 503-509.

Saxe, R., Brett, M. and Kanwisher, N. (2006). Divide and conquer: in defense of functional localizers. NeuroImage, 30, 1088-1096.

Tomonaga, M. (1994). How laboratory-raised Japanese monkeys (Macaca fuscata) perceive rotated photographs of monkeys: Evidence for an inversion effect in face perception. Primates, 35, 155-165.

Tomonaga, M. (2007). Visual search for orientation of faces by a chimpanzee (Pan troglodytes): face-specific upright superiority and the role of facial configural properties. Primates, 48, 1-12.

Valentine, T. (1988). Upside-down faces: a review of the effects of inversion upon face recognition. Brit. J. Psychol., 79, 471-491.

Vermeire, B. A. & Hamilton, C. R. (1998). Inversion effect for faces in split-brain monkeys. Neuropsychologia, 36, 1003-1014.

Watson, C. C., Newport, D. & Casey, M. E. (1996). A single-scatter simulation technique for scatter correction in 3D PET. In: Fully Three Dimensional Image Reconstruction in Radiology and Nuclear Medicine (Ed. by Grangeat, P. & Amans, J. L.), pp. 255-268: Kluwer Academic Publishers.

Weiss, D. J., Kralik, J. D. & Hauser, M. D. (2001). Face processing in cotton-top tamarins (Saguinus oedipus). Anim. Cog., 4, 191-205.

Figure S1. An Example of a Matching-to-Sample Trial Showing Chimpanzee Faces (Face Task) and Clip Art Objects (Object Task)

Subjects first contact the sample stimulus, the one to be matched, at the top of the screen using a joystick controlled cursor (cross). They then must select one of the two comparison images located at the bottom of the screen that matches the sample (bottom right and left, respectively).

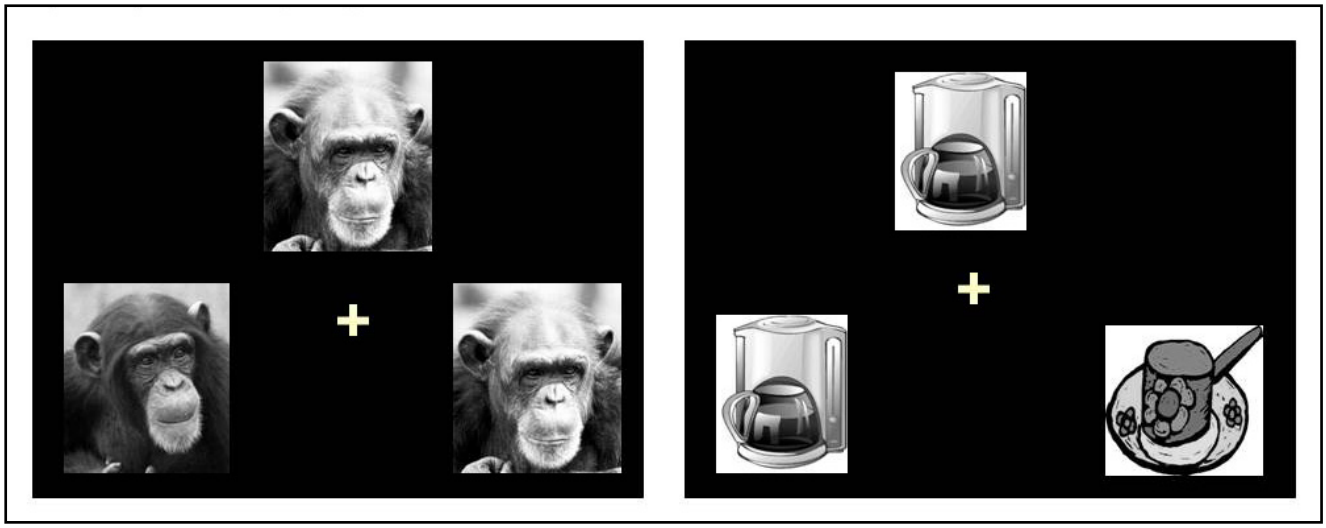

Figure S2A. An Illustration of the Fusiform Gyrus ROI

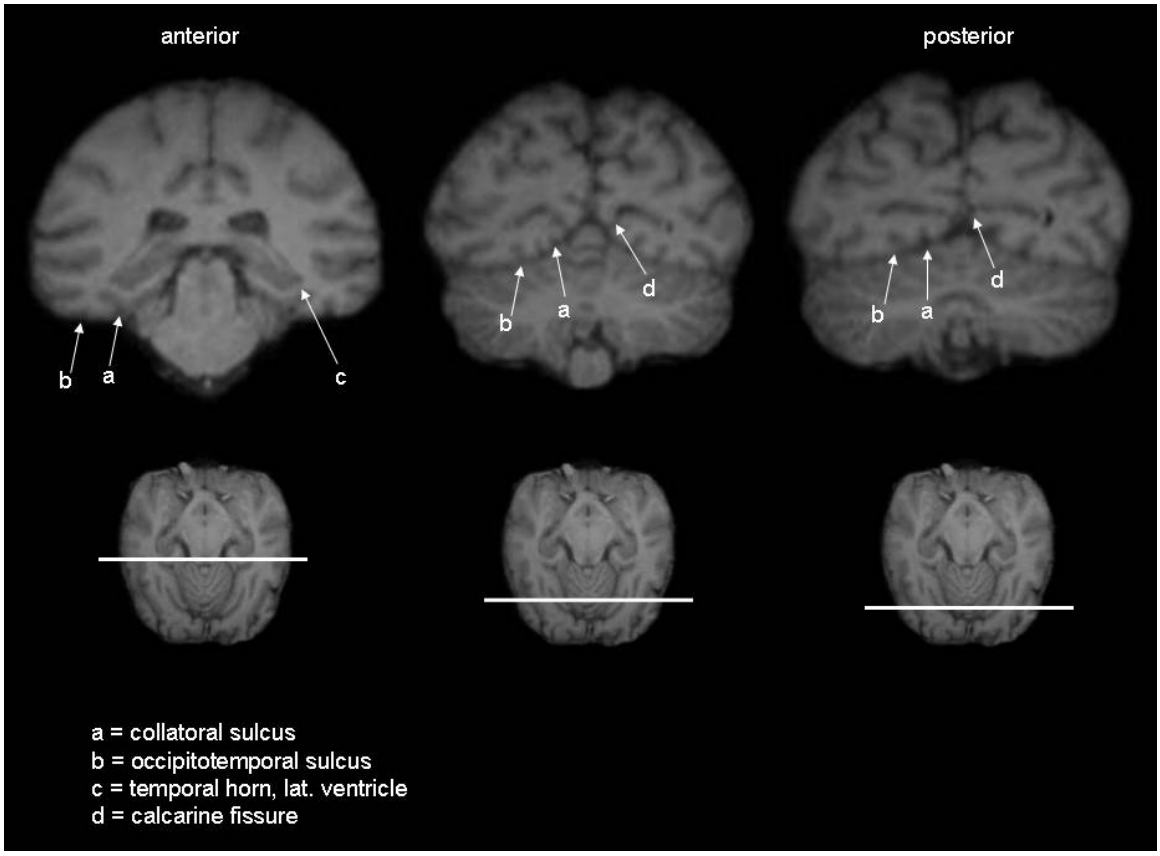

Figure S2B. An Illustration of the Posterior STS ROI

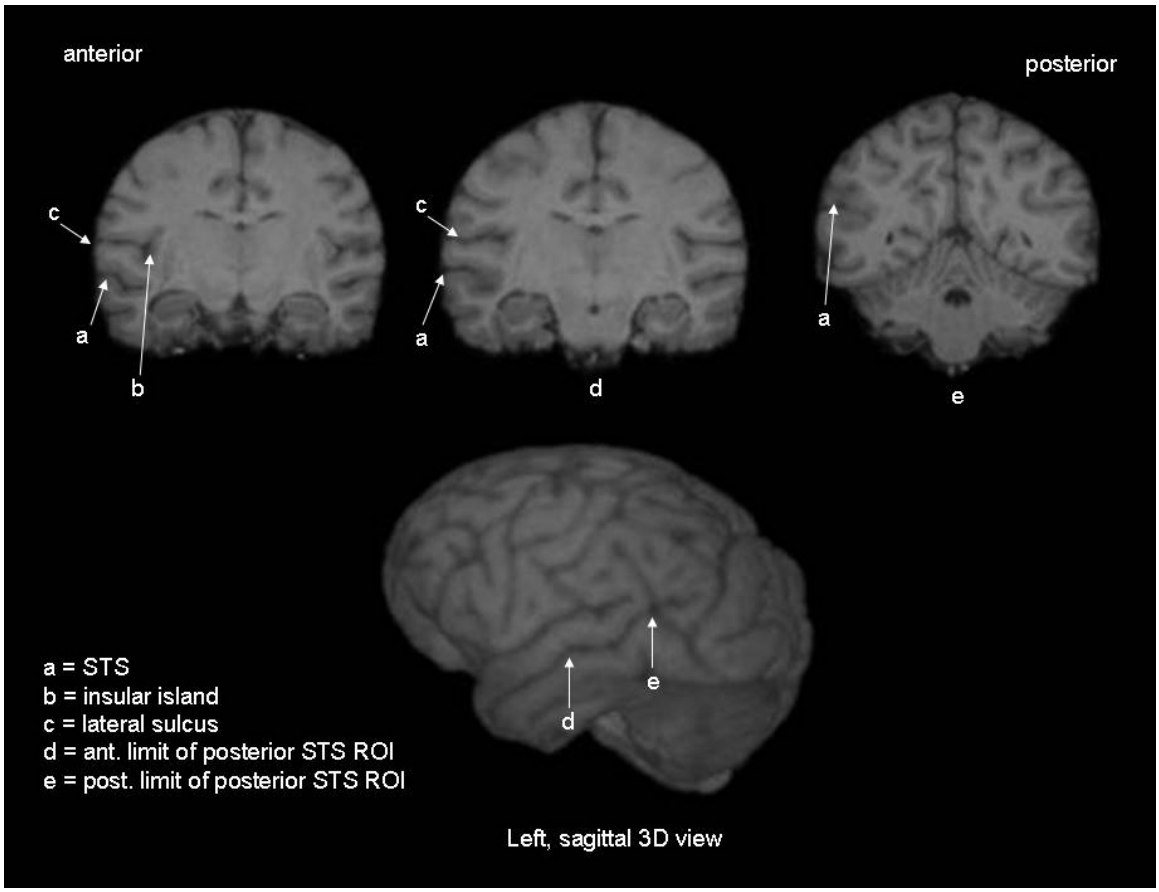

Figure S3. Two Ventral Views Showing Three-Dimensional Renderings of the MNI152 Human Template Brain with the Cerebellum Removed

Translucent probabilistic masks from the Harvard-Oxford Cortical Atlas are overlaid on the fusiform gyrus, thresholded at 25%. Color-coded regions of the fusiform gyrus are: red, anterior temporal; yellow, posterior temporal; green, temporal-occipital; blue, occipital. Figure S2A plots the location of individual fusiform face areas (FFAs) reported in [2], and Figure S2B plots the centroids for FFAs reported from 17 published studies on human face processing (see references below). These are plotted using their Talairach coordinates converted to MNI coordinates and show the large variability in the location of FFAs reported both within subjects and between studies.

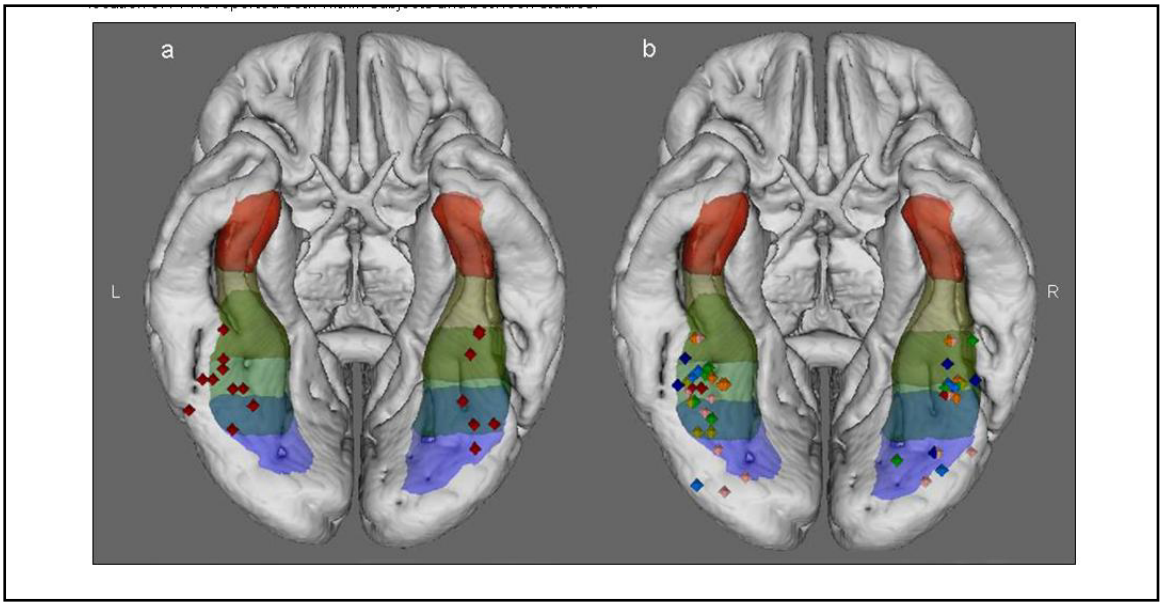

Figure S4. The Top 5% of Face-Selective Voxels (Face > Object) Shown in the Fusiform Gyrus of Each Individual Subject

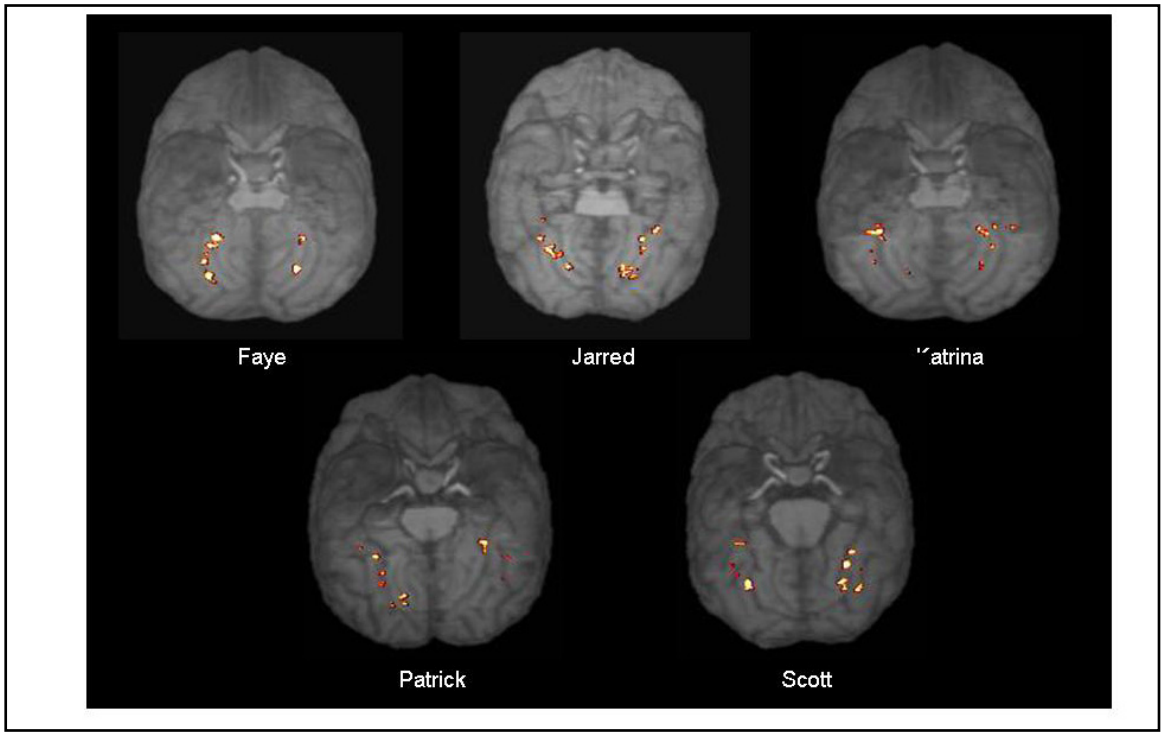

Figure S5. Calculated Gray Matter Tissue Absorption Curve after Oral Dose of [18F] FDG

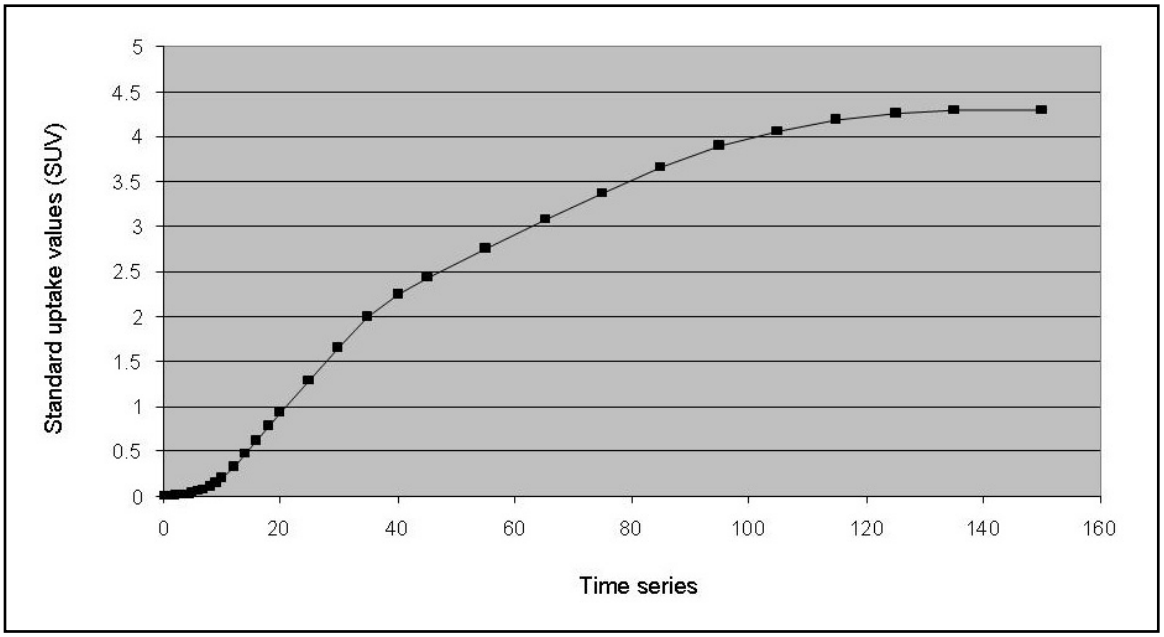

Figure S6. An Anesthetized Chimpanzee in a Position Emission Tomography Scanner